

# Surface Tension and Surface Dilatational Elasticity of Associating Hydrophobically Modified Polyacrylamides in Aqueous Solutions

Hilde Beate Molvig Kopperud and Finn Knut Hansen\*

Department of Chemistry, University of Oslo, P.O. Box 1033 Blindern, N-0315 Oslo, Norway

Received December 7, 2000; Revised Manuscript Received April 11, 2001

**ABSTRACT:** The effects of the variation of different parameters in some hydrophobically modified polyacrylamides in aqueous polymer solution on their surface properties have been investigated. Two different hydrophobes, *N,N*-dihexylacrylamide (DiHexAM) and *N*-(4-butylphenyl)acrylamide (BPAM), have been used; the former was most extensively investigated. The molecular weight (50 000–1 000 000), amount of hydrophobes (0.5–2 mol %), and block length of the hydrophobic groups (1–7 units) have been varied. The dynamic surface pressure has been measured by means of drop shape analysis of a sessile bubble, and the surface dilatational elasticity and viscosity have been obtained during the adsorption process by the oscillating bubble technique.  $\Pi$ – $A$  isotherms of the adsorbed polymers have also been measured by using compression and decompression cycles on the sessile bubble. All the hydrophobically modified polymers show surface activity, but the adsorption rate is very low; it usually takes more than 24 h to obtain surface pressures beyond 20 mN m<sup>-1</sup>. The adsorption is therefore believed to be controlled by unfolding and reconfiguration of the bulk polymer and the penetration of the surface layer by individual hydrophobic blocks. Adsorption rate generally decreases with increasing molecular weight, except where a synergistic effect is believed to be present. Increasing block length (keeping the amount of hydrophobe constant) leads to a lower adsorption rate, while increasing amount of hydrophobe (keeping the block length constant) has the opposite effect. The assumption of the penetration of individual hydrophobic blocks into the surface layer accounts for both these effects. All polymers show high surface dilatational elasticity, up to ca. 80 mN m<sup>-1</sup>, and almost zero surface viscosity. The surface elasticity as a function of the surface pressure follows a linear relationship over practically all the surface pressure range with an average slope of 3.6. This agrees well with a theoretical derivation based on scaling theory, and it is thus possible to calculate the  $\nu$  exponent for the polymers at the interface. An average of 0.69 is obtained, which shows that the surface layer is a medium to good solvent for the block copolymer.

## Introduction

The interest in associating polymers has been great the past decade due to their interesting solution behavior.<sup>1–14</sup> They are important additives in environmentally friendly formulations of paints and lacquers and are promising ingredients for oil production and transport and in medical formulations.<sup>2,3,5,15,16</sup> The major types of associating polymers include hydrophobically modified poly(oxyethylene) (HEUR, Pluronic etc.), different types of modified cellulose (HEC, EHEC), and hydrophobically modified poly(acrylic acid) (PAA) and polyacrylamide (PAM). The bulk solution properties of these different types of associating polymers have been extensively studied, and experimental methods such as rheology and different scattering techniques have been applied. Although adsorption of these polymers to both solid and liquid surfaces is an important behavior in colloidal products, surface properties of these substances have been given less attention.<sup>17</sup> In this laboratory we have investigated the adsorption dynamics and surface dilatational elasticity of EHEC and some other polymers at the air/water interface by means of axisymmetric drop shape analysis.<sup>18–20</sup> This technique has been proven very efficient in revealing important information on the surface properties both of pure polymers and of polymer–surfactant interfacial interaction.

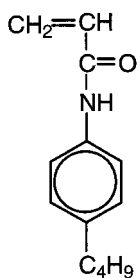
The nonionic water-soluble copolymers of acrylamide prepared with hydrophobic comonomers (HM–PAM)

have attracted a great deal of interest.<sup>6–8,10,11,21–23</sup> Although the acrylamide homopolymer is very water-soluble, only small amounts (a few percent) of hydrophobic modification changes the solubility dramatically. In aqueous solution, above the overlap concentration of the polymer chains, the hydrophobic groups form intermolecular hydrophobic associations, resulting in a strong increase in solution viscosity. Several studies of the solution properties of these polymers have been published.<sup>10,24–26</sup> In contrast to many water-soluble polymers, acrylamide shows practically no surface activity. However, it would be expected that hydrophobic modification would change also this property. Preliminary measurements with a ring tensiometer<sup>25</sup> showed that if at all surface active, these polymers are adsorbing very slowly to the air/water interface. The development of our instrument for automatic drop shape analysis has allowed the measurement of dynamic surface tensions and surface dilatational elastic properties of slowly adsorbing polymers, and the instrument is therefore well suited for the investigation of PAM systems. In the present work the surface properties of two slightly different types of hydrophobically modified PAM have been studied by drop shape analysis of a sessile bubble. Both the amount of hydrophobic modification and the block length of the hydrophobe have been varied, and the polymer has been investigated regarding both rate of adsorption and surface elasticity.

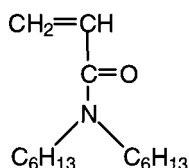
## Experimental Section

**Materials and Sample Preparation.** The structures of the two different comonomers are shown in Figure 1.

\* Corresponding author. Tel +47-22855554; fax +47-22855542; e-mail f.k.hansen@kjemi.uio.no.



N-(4-butylphenyl)acrylamide  
BPAM



N,N-dihexylacrylamide  
DiHexAM

**Figure 1.** Chemical structure of the comonomers BPAM and DiHexAM.

**Table 1.** Characteristic Data of the Copolymers

sample	mol wt ( $\times 10^{-3}$ )	comonomer	[H] (mol %)	block length
05M2D3.2	42	DiHexAM	2	3.2
1M1D3.2	115	DiHexAM	1	3.2
1M2D3.2	140	DiHexAM	2	3.2
1M2D7	160	DiHexAM	2	7
5M05D3.2	450	DiHexAM	0.5	3.2
5M1D3.2	420	DiHexAM	1	3.2
5M1D5	450	DiHexAM	1	5
5M1D7	460	DiHexAM	1	7
MR40	1150	DiHexAM	2	3.2
BPAM-PAM	190	BPAM	1	1
PAM	360	none	0	0

All samples but BPAM-PAM and PAM were polyacrylamides hydrophobically modified with *N,N*-dihexylacrylamide (DiHexAM) and were kindly provided by F. Candau. The use of disubstituted acrylamides (rather than monosubstituted acrylamides) was shown to lead to samples homogeneous in composition.<sup>10</sup> The synthesis and characterization of these copolymers are reported elsewhere.<sup>10,26</sup> The copolymer modified with the monosubstituted acrylamide *N*-(4-butylphenyl)acrylamide (BPAM) was previously synthesized and has been described elsewhere.<sup>24</sup> This polymerization procedure is also considered to yield a copolymer of homogeneous composition with a random distribution of hydrophobic units in the hydrophilic backbone. The polymerization of a reference pure PAM is also described.<sup>24</sup> Some characteristic data of all the polymers are shown in Table 1.

All samples for surface tension measurements were prepared by weighing the appropriate amounts of dry polymer and water, swelling, and dissolving the polymer by stirring and then letting the solutions equilibrate for several days. The polymer solution was then added to a quartz cuvette, which was placed in a thermostated chamber in the Drop instrument. All glass equipment was thoroughly cleaned by chromic sulfuric acid, and all water was ion exchanged followed by distillation in a glass still. The water was checked by measuring the surface tension during an extended time period by the sessile bubble technique. The decrease in surface tension was less than 0.5 mN m<sup>-1</sup> in 24 h.

**Instruments.** The instrument for drop shape analysis has been described elsewhere<sup>18</sup> and is only briefly reviewed here. The instrument consists of a goniometer (Ramé-Hart) fitted with a macro lens and a CCD video camera. The video frames are captured by a frame grabber in a PC that also controls the drop volume through a drop control unit. This consists of a dispenser and an oscillation unit with a syringe with an excenter-mounted piston that is driven by a stepper motor. The units are mounted in series with water-filled tubes. The drops and bubbles are extended from the tip of a small PTFE tube into a quartz cuvette inside a thermostated and water-filled environmental chamber with glass windows. The PTFE tube contains an air pocket toward the water in the tube.

**Data Analysis.** The DROPimage computer program controls the instrument and measurement sequences and per-

forms calculations. The instrument measures the drop dimensions (height, width, area, and volume) as well as the surface tension by the drop shape method described earlier.<sup>27,28</sup> The measurement of surface dilatational modules by means of axisymmetric drop shape analysis combined with the oscillating bubble technique has also been outlined elsewhere<sup>18</sup> and will only be briefly reviewed here. The theoretical foundation for the measurement of surface rheological properties is well established.<sup>29-31</sup> The surface elasticity,  $E$ , follows the definition given by Gibbs, but as many surfaces both contain an elastic and a viscous component, the term "surface dilatational modulus" has been used for this more general case. The contribution of the elastic and viscous terms depend on the different types of relaxation processes that occur in the surface layer and on the interaction of the surface with its surroundings, i.e., with the bulk liquid(s). For an oscillating bubble, we vary the surface area by changing the bubble volume in a sinusoidal manner with a frequency  $\omega$ . This results in a corresponding sinusoidal variation in the bubble surface area, provided that the volume change is small. This also leads to a corresponding surface tension variation. We can write this

$$\Delta A = A - A_0 = A_a \sin(\omega t) \quad (1)$$

$$\Delta\gamma = \gamma - \gamma_0 = \gamma_a \sin(\omega t + \delta) \quad (2)$$

Here  $A_a$  is the area amplitude and  $A_0$  is the equilibrium surface area,  $t$  is the time,  $\gamma_a$  is the measured amplitude,  $\gamma_0$  is the equilibrium surface tension, and  $\delta$  is the phase angle. In the usual manner, the (complex) surface dilatational modulus,  $E^*$ , is then expressed by

$$E^* = E' + iE'' = |E| \cos \delta + i|E| \sin \delta \quad (3)$$

where

$$|E| = \frac{\gamma_a}{A_a/A_0} \quad (4)$$

The storage modulus,  $E'$ , will be equal to the pure elastic contribution, and  $E''$  will be proportional to the viscous contribution with

$$E'' = \eta_d \omega \quad (5)$$

Here  $\eta_d$  is the surface dilatational viscosity. The measured surface area and surface tension data as a function of time are analyzed by fitting sine functions by means of a nonlinear curve-fitting (Marquard) algorithm.

**Experimental Procedure.** A dynamic surface tension measurement is started by a programmed rapid bubble formation, immediately followed by data acquisition. Recent improvements of the DROPimage software allow for simultaneous measurements of the dynamic surface tension and dilatational surface moduli. If adsorption is sufficiently slow, oscillation experiments may be performed during the adsorption period, and this implies that the study of the elasticity as a function of surface tension (or pressure) can be done easily. At least two parallels of the dynamic surface tension curves ( $\gamma$  vs time) were performed in order to ensure reproducibility of the results. Usually two or three parallels were measured for the surface dilatational moduli through the frequencies investigated (0.2–1.8 Hz). The results had good reproducibility. For measurements at low surface pressure when the surface tension was changing rapidly, only one oscillation sweep was performed. Reproducibility was also checked by measuring with both increasing and decreasing frequency sweeps. No differences were detected between the separate sweeps.

At the maximum time for the adsorption measurement, compression/decompression experiments were performed. This implies that the drop volume was changed in steps by the instrument both downward and upward from the equilibrium volume. For each step, the volume, surface area and surface

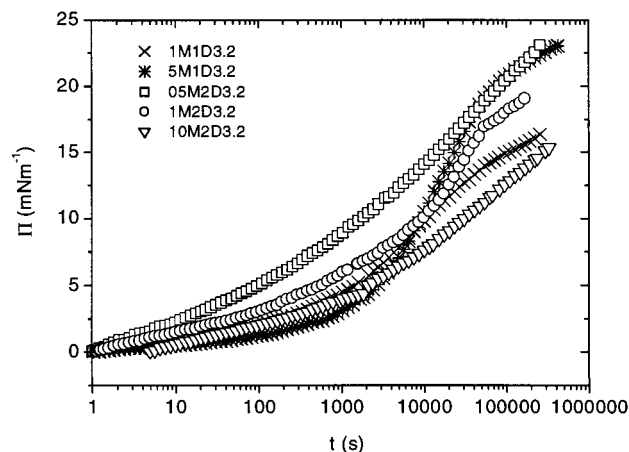


**Figure 2.** Surface pressure  $\Pi$  as a function of time  $t$  for the polymers indicated.

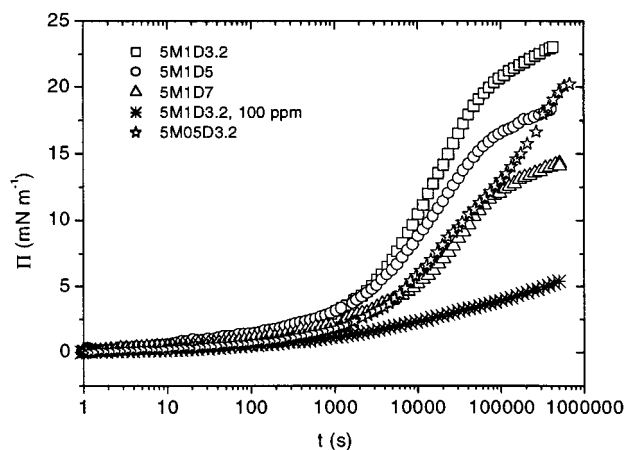


**Figure 3.** Surface pressure  $\Pi$  as a function of time  $t$  for the polymers indicated.

tension were measured. This procedure simulates the movement of the barriers in a Langmuir surface balance, and although absolute molecular areas cannot be obtained, a relative  $\Pi$ - $A$  isotherm may be plotted, assuming there is no adsorption or desorption at the surface.

## Results and Discussion

**Adsorption and Dynamic Surface Tension.** The surface pressure of pure PAM is generally very low, due to the strong hydrophilic nature of the polymer. The surface tension has previously been found to be independent of molecular weight and polymer concentration (up to 1% w/w) with an average value of  $69.15 \text{ mN m}^{-1}$  at  $25^\circ\text{C}$ .<sup>32,33</sup> This means that the surface pressure,  $\Pi$ , is ca.  $3 \text{ mN m}^{-1}$ . The results from the present work do not differ essentially from this, although the question of equilibrium always arises in such systems. An "equilibrium" value of  $\Pi \approx 4 \text{ mN m}^{-1}$  at very long times has been obtained here (Figure 4). The incorporation of hydrophobic groups onto the hydrophilic polymer backbone, however, changes this behavior of very low surface activity. In Figures 2–4 are shown the dynamic surface pressure curves ( $\Pi$  as a function of time) for the different polymers investigated. Although the hydrophobic modification changes the surface activity of the polymers, the rate of increase in the surface pressure is still quite low. Also, equilibrium adsorption was not obtained in any of these systems even when measurements were conducted for time periods of up to 1 week. Adsorption of polymers is generally considerably slower

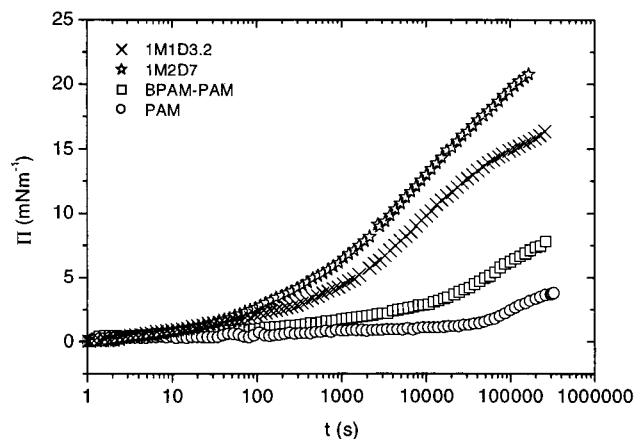


**Figure 4.** Surface pressure  $\Pi$  as a function of time  $t$  for the polymers indicated.

than that of simple surfactants, but these polymers are adsorbing even slower than others we have investigated. For instance, EHEC at the same bulk concentration (1000 ppm) attains a surface pressure of  $>17 \text{ mN m}^{-1}$  in less than 1 s.<sup>18</sup> However, the surface pressures of these HM-PAMs obtained after long times are not lower than that of EHEC (rather the opposite). The fact that the molecular weights of these polymers are higher than that of EHEC cannot compensate for the big difference in rate and indicates that the adsorption mechanism is different from that of e.g. EHEC.

The very slow increase in the surface pressure indicates that the adsorption of the HM-PAMs is not diffusion-controlled but more likely controlled by unfolding and reorientation of the polymer molecules at the surface and by subsequent adsorption of the single hydrophobic blocks. This means that the polymer concentration is constant all the way up to the subsurface (just below the surface layer), and the slow adsorption from the subsurface means that there are very pronounced conformation changes upon adsorption and that the activation energy for adsorption is very high. When considering the effects of the molecular weight and structure on the rate of adsorption (or, more precisely, the rate of surface pressure increase), one must consider both the bulk and the surface conformation of the polymer. As mentioned in the Introduction, these polymers form intermolecular associations in solution, dependent on concentration, and they also form intramolecular associations that are more pronounced in dilute solutions. The adsorption process will require breakage of at least some of these associations, and the rate of adsorption may be dependent also upon this process. At the surface, the polymer may possess different conformations, dependent on both concentration and polymer structure. At the low polymer concentrations used in this work, there is very little intermolecular association, but intramolecular associations are probably present.

Further arguments concerning the adsorption mechanism is given in the Appendix. It is concluded that adsorption of the molecules takes place one hydrophobic block at the time and that this is one important rate-determining step. Consequently, hydrophilic loops and tails of the polymer are extended into the solution, and these chains may also contain hydrophobic blocks that subsequently are slowly adsorbed. Presuming such a mechanism, the effect of hydrophobic substitution, block length, and other variables on the adsorption rate may



be evaluated. When looking at the data presented below, one should also bear in mind that equal surface pressures of two polymers does not automatically mean that the surface concentrations are the same, because this depends on the adsorption energy and conformation of the surface layer. It may, however, mean that the concentration of hydrophobic species is mostly the same.

Most of the measurements were performed at a concentration of 1000 ppm. This avoids much of the intermolecular associations and gives sufficient time for oscillation experiments during adsorption. When the polymer concentration is decreased, the surface pressure shows a slower increase as expected. Similar results have been seen for instance for the cellulose derivative EHEC in aqueous solution.<sup>18</sup>

The curves in Figure 2 show the effect of molecular weight for the xM1D3.2 and xM2D3.2 polymers (1% and 2% substitution, respectively, mean block length of 3.2; see Table 1). An increase in the molecular weight for the 2% substituted polymers (from  $5 \times 10^4$  to  $1 \times 10^6$  g mol<sup>-1</sup>) results in a lower rate of adsorption. The same is the case for the 1% substituted polymer at short times, but this trend is reversed at longer times (>20.000 s) where the sample with the highest molecular weight shows the highest surface pressure. It may be speculated that the reason for this behavior may be found in the complex interplay between intramolecular associations in the solutions and adsorption to the surface. Why this should be more pronounced for the 1% than for the 2% substituted polymer, however, is not easy to understand. Another more probable explanation of the reversed trend of the 5M1D3.2 polymer may be found in the postulated adsorption mechanism of adsorption of single hydrophobic blocks and the synergistic effect: As the number of hydrophobic blocks increases proportional to the molecular weight, a high molecular weight polymer with some of the blocks already adsorbed will contain more blocks close to the surface. It may be postulated that this facilitates the total transport of blocks to the surface, resulting in a higher rate of adsorption. This synergistic effect would be expected to be important only when a lot of the blocks already are adsorbed, i.e., at higher surface pressures, as observed. Generally, it is seen that the effect of molecular weight is not very great, which again indicates that diffusion is not the rate-limiting step.

The effect of changing the hydrophobic block length is illustrated in Figure 3, where all the polymers are of the same molecular weight ( $5 \times 10^5$ ). It seems clear that increasing the block length gives a slower increase of the surface pressure. This result may be explained by considering the intramolecular associations of these polymers in bulk. This association increases with increasing block length, resulting in longer disengagement times for the hydrophobic groups upon adsorption as the lifetime of an association is believed to be controlled by the block length.<sup>26</sup> It may be expected that a longer hydrophobic block would make the polymer more hydrophobic and thus increase adsorption, but in these polymers the increase in hydrophobic block length is accompanied by a simultaneous increase in the hydrophilic block length (other variables are kept constant), and the total hydrophobicity of the molecule stays constant. Another important effect of a longer hydrophobic block is connected to the penetration of the surface layer, as described in the Appendix. Over a quite large range in surface pressure (ca. 3–15 mN m<sup>-1</sup>) the

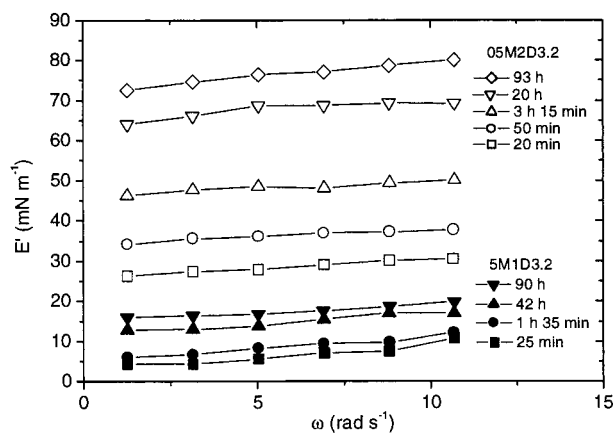


**Figure 5.** Elastic modulus  $E'$  as a function of the oscillation frequency  $\omega$  for the two copolymers 05M2D3.2 (open symbols) (at 1000 ppm) and 5M1D3.2 (closed symbols) (at 100 ppm) at different times as indicated.

activation energy of adsorption is proportional to the product  $\Pi A$  where  $A$  is the specific surface area of a hydrophobic block. Compared at the same surface pressure,  $\Pi$ , the polymer with the longer blocks will have the highest activation energy and therefore adsorb more slowly. For shorter polymeric chains an increased mobility may hide this effect as shown from the samples 1M2D3.2 (Figure 2) and 1M2D7 (Figure 4).

Increasing the amount of hydrophobe, keeping the molecular weight and hydrophobic block length constant, gives a faster increase in the surface pressure. This conclusion is reached by comparing the curves for 1M1D3.2 (Figure 4) and 1M2D3.2 (Figure 2) and those for 5M05D3.2 and 5M1D3.2 (Figure 3). The effect is stronger in the latter case, again indicating a synergistic effect as outlined above.

The two hydrophobic comonomers used in this work differ in being a mono- (BPAM) or a disubstituted (DiHexAM) acrylamide, as well as in the type of hydrophobic chain, phenyl- $C_4H_9$  and  $C_6H_{13}$ , respectively (Figure 1). The latter is clearly more hydrophobic than the former, and very low and slow surface activity is seen for the BPAM copolymer (a decrease of ca. 5 mN m<sup>-1</sup> in 1 week, Figure 4). This polymer was therefore only measured at a concentration of 5000 ppm and still showed slower adsorption behavior than all the DiHexAM copolymers at 1000 ppm. The great difference might be due to extra polymer–polymer hydrogen bonds in the proximity of, and induced by, the hydrophobic aggregation which is possible for the BPAM copolymer (monosubstituted) but not for the DiHexAM copolymer (disubstituted).

**Surface Elasticity.** Typical plots of the elastic modulus,  $E'$ , vs angular frequency and at different times are shown in Figure 5 for two different samples. The low molecular weight sample, 05M2D3.2, which adsorbs relatively fast, exhibits elastic moduli ranging from 25 to 80 mN m<sup>-1</sup> during the time of the adsorption experiment. On the other hand, the 5M1D3.2 sample with a higher molecular weight and lower hydrophobic substitution, but at a concentration of 100 ppm, only exhibits moduli in the range 5–15 mN m<sup>-1</sup> during the same period of time. Both samples show very low frequency dependence. The corresponding loss modules,  $E''$ , are all very low, <5 mN m<sup>-1</sup>, and not frequency dependent (not shown). This general trend is typical for all samples of these polymers. The frequency dependency of  $E'$  and  $E''$ , as well as the presence of  $E''$ , is

generally believed to be caused by relaxation processes in the interface.<sup>30,31,34</sup> The almost independence of  $E'$  of frequency combined with the low values of  $E''$  therefore means that such processes are negligible in these systems. The two types of relaxation processes usually considered are the exchange of matter between the bulk solution and the interface and conformational changes in the interface. That the former process is absent in these systems may be expected from the very slow adsorption kinetics and the lack of an adsorption equilibrium which means that there is very little desorption, too. The second process, in-surface relaxation, is also practically absent and means that these polymer layers are almost purely elastic. As a 3-D analogue, they may be compared to the rheological properties of a stiff crystalline polymer that also has a very high and almost frequency-independent storage module and a low loss module.<sup>35</sup>

The typical dependence of the surface elasticity of these polymers on the surface pressure is shown in Figure 6. The figure shows a plot of  $E'$  and  $E''$  vs  $\Pi$  for two different frequencies (0.2 and 1.7 Hz) for the sample 5M1D5. Linear fits to the data are shown, and it is observed that both  $E'$  and  $E''$  data are quite well described by a straight line. Similar results are also obtained for the BPAM copolymer and the pure PAM polymer as shown in Figure 7. This linear relationship invites to describing the dependence of the surface pressure on surface concentration by means of a scaling expression:<sup>36</sup>

$$\Pi \sim \Gamma^y \quad (6)$$

This expression is the 2-dimensional analogue of the well-known scaling theory for semidilute polymer solutions. In this context, the scaling exponent  $y$  is given by

$$y = \frac{d\nu}{d\nu - 1} \quad (7)$$

where  $d$  is the dimensionality, in this case 2, and  $\nu$  is the critical exponent of the excluded volume. Gibbs' expression for the (static) surface elasticity is

$$E_0 = -\frac{d\Pi}{d \ln A} = \frac{d\Pi}{d \ln \Gamma} \quad (8)$$

By taking the derivative of eq 6 and inserting in eq 8, we obtain<sup>37</sup>

$$E_0 = y\Pi \quad (9)$$

It should be noted that the elasticity expressed by  $E_0$  is the Gibbs elasticity, which may be different from  $E'$ , rather  $E_0 = E'(\omega \rightarrow \infty)$ . In our case, however, when  $E'$  is almost independent of frequency and  $E''$  is very low, we may use  $E'$  for  $E_0$ . The constant  $\nu$  may be interpreted as a measure of the thermodynamic conditions in the surface system<sup>38</sup> and is expected to vary from ca. 0.51 under  $\Theta$ -conditions to 0.77 in a good solvent.<sup>37</sup> Supposing  $d = 2$ , which is probably a good approximation for a flat configured surface layer, the value of  $y$  is expected to vary between a quite high value (up to ca. 50) for  $\Theta$ -conditions to 2.85 for a good solvent. Using eq 9, we see that the scaling theory predicts a linear relationship between  $E_0$  ( $\approx E'$ ) and  $\Pi$  with  $y$  equal to the slope. This seems to fit our data quite well, and the slope of  $E'$  vs

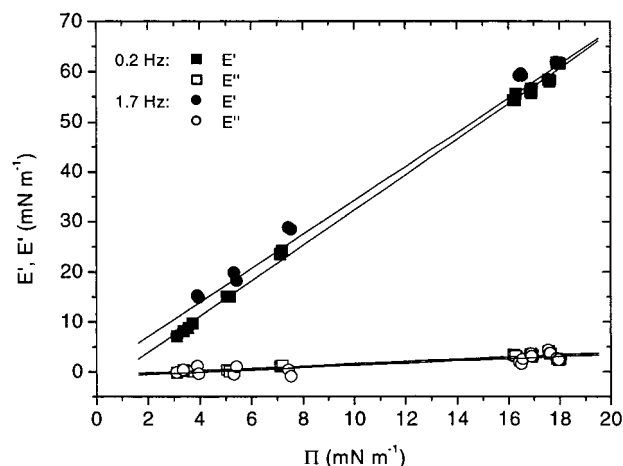


**Figure 6.** Surface dilatational elastic  $E'$  (closed symbols) and viscous  $E''$  (open symbols) moduli as a function of the surface pressure  $\Pi$  for the copolymer 5M1D5 (1000 ppm) at two different oscillation frequencies: 0.2 Hz (squares), 1.7 Hz (circles). Lines are least-squares fits to the data.

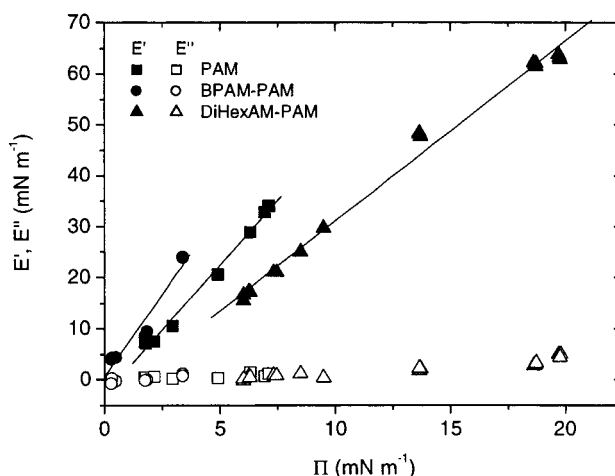


**Figure 7.** Surface dilatational elastic  $E'$  (closed symbols) and viscous  $E''$  (open symbols) moduli as a function of the surface pressure  $\Pi$  for pure polyacrylamide and copolymers with the two different modifications as indicated. Lines are fits to the data.

$\Pi$  in Figure 6 is found to be  $3.55 \pm 0.03$  (at 0.2 Hz). Figure 8 shows all the measured values of  $E'$  at different surface pressures for all the samples based on the DiHexAM comonomer. It is seen that they all fall more or less onto the same line regardless of molecular weight, hydrophobic block length, etc., but that there are small differences between the samples. It is not completely certain whether these differences are significant, but they are probably so. For instance, the 5M1D7 sample seems to be higher than the others, while the low substituted 5M05D3.2 is at the lower end. The values of  $y$  have been calculated for all the individual samples and are shown in Table 2 together with the calculated values of  $\nu$ . We see that  $y$  varies from 3.06 to 4.34 for the DiHexAM copolymers, with a corresponding value of  $\nu$  from 0.74 to 0.65. This should mean that the air/water interface is a medium to good solvent for all these polymers. If we also consider the results for the polymer based on the BPAM comonomer and the pure PAM polymer, we see that the values of  $y$  are higher and the corresponding value of  $\nu$  lower; down

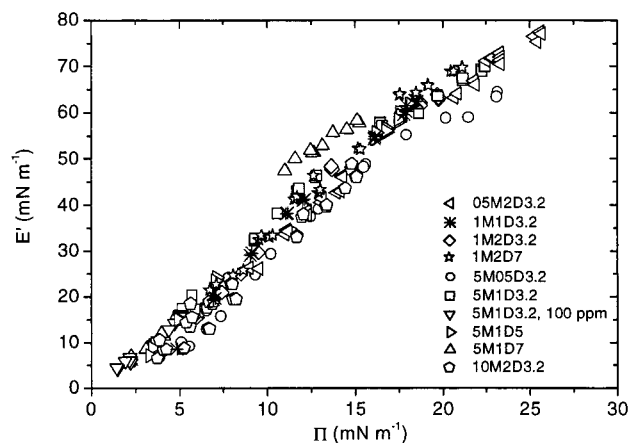


**Figure 8.** Elastic modulus  $E'$  as a function of the surface pressure  $\Pi$  for all the DiHexAM copolymers as indicated.

**Table 2.** Scaling Parameter  $\gamma$  and the Excluded-Volume Parameter  $\nu$  for Different Samples

sample	$C$ (ppm)	$\gamma$	$\nu$
05M2D3.2	1000	3.06	0.74
1M1D3.2	1000	3.87	0.67
1M2D3.2	1000	3.53	0.70
1M2D7	1000	3.50	0.70
5M05D3.2	1000	3.72	0.68
5M1D3.2	1000	3.67	0.69
5M1D3.2	100	3.23	0.72
5M1D5	1000	3.55	0.70
5M1D7	1000	4.35	0.65
MR40	1000	3.60	0.69
BPAM-PAM	5000	5.07	0.62
PAM	5000	6.43	0.59

to 0.59 for pure PAM. The excluded-volume parameter can also be found from<sup>39</sup>

$$\nu = \frac{a + 1}{3} \quad (10)$$

where  $a$  is the Mark-Houwink exponent. From reported values of the Mark-Houwink exponent, the excluded-volume parameter for PAM in water (bulk solution) ranges from 0.55 to 0.61 at 25 °C, which is well in line with the value of 0.59 found here. We see that hydrophobic modification increases the value of  $\nu$  in the surface layer and more with the DiHexAM comonomer than with BPAM. An increased hydrophobicity therefore leads to better solution properties in the surface layer.

A small comment may be added to the fact that many of the  $E'$  vs  $\Pi$  plots do not seem to go through the origin. Theoretically, at very low surface concentrations, a surface layer is usually considered to be in the gaseous state. For many polymers, the limit for this state may be at surface pressures well below 1 mN m<sup>-1</sup>.<sup>36</sup> For a gaseous layer, the equation of state is

$$\Pi A = RT \quad \text{or} \quad \Pi = RT/\Gamma \quad (11)$$

Inserting this into eq 8, we end up with  $E_0 = \Pi$ , which means that the slope of  $E_0$  vs  $\Pi$  at low surface pressures should be 1. The curves based on scaling theory are therefore not expected to go through the origin but may come quite close for high molecular weight polymers. Another, more trivial, reason for the inability of the curves to go through the origin is of course small errors in  $\Pi$ .

**Compression/Decompression Measurements.** By changing the drop volume in small steps with simulta-

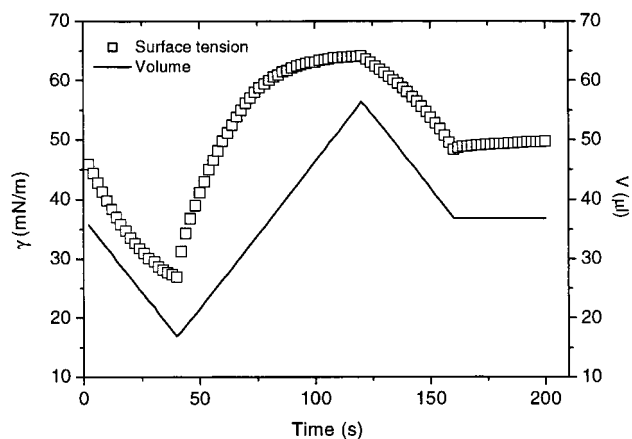


**Figure 9.** Bubble volume  $V$  (right) and corresponding surface tension  $\gamma$  (left) as a function of time  $t$  for the copolymer 05M2D3.2 from a compression/decompression experiment.

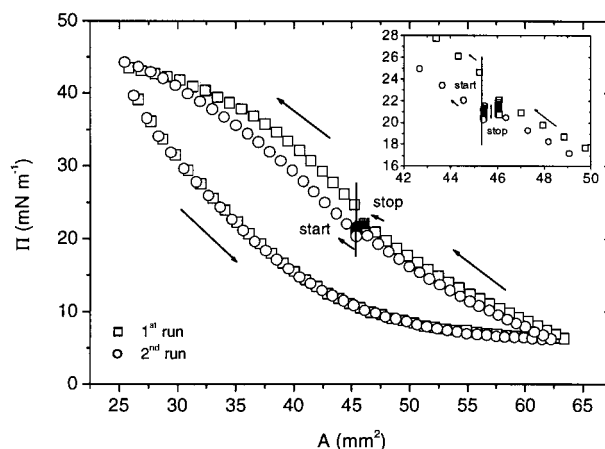


**Figure 10.** Surface tension  $\gamma$  as a function of the bubble surface area  $A$  for the copolymer 05M2D3.2 from a compression/decompression experiment. Starting point is at the vertical bar, first decreasing, then increasing, and again decreasing area as indicated by the arrows.

neous drop shape analysis, a simulation of a compression/decompression cycle in a Langmuir surface balance may be created. From the resulting data, a  $\Pi$ - $A$  isotherm may be constructed, except that the molecular surface area is not obtained because the absolute surface concentration is unknown. Such measurements were performed at the highest surface pressure obtained for the different samples, i.e., closest to the "equilibrium" value. The measurements were performed by subsequently decreasing and increasing the drop volume by 0.5 or 1  $\mu$ L each 2 s in a sawtooth fashion, ending again at the initial drop volume. A typical plot of the drop volume and corresponding surface tension of sample 05M2D3.2 is shown in Figure 9. The surface tension does not follow the same linear sawtooth shape as the volume as the compression and decompression curves are different because of hysteresis. By plotting the surface pressure as a function of surface area, a  $\Pi$ - $A$  isotherm is constructed. Figure 10 shows the resulting isotherm for two subsequent compression/decompression experiments of the same sample. The starting point of the measurements is in the middle of the figure (indicated by a vertical line), and the arrows indicate the direction of the run. As can be seen, the starting point of the second run deviates from that of the first run, but the decompression curves from the two runs fall on top of each other. If more repetitions of the compression/



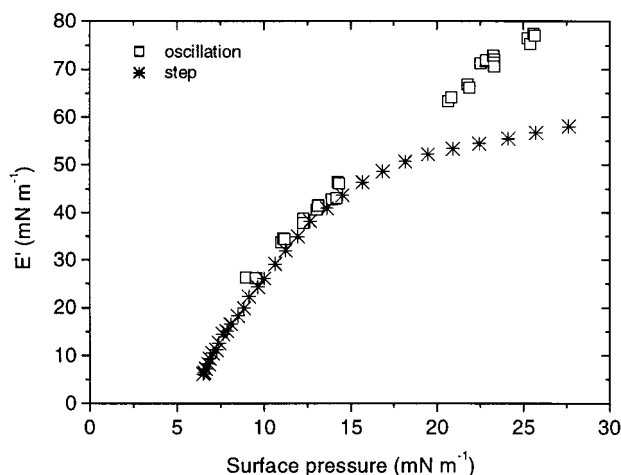


**Figure 11.** Surface dilatational elasticity measured from bubble oscillations ( $\square$ ) and calculated from compression–decompression measurements (\*). Sample 05M2D3.2.

decompression cycle are done immediately, the subsequent data are the same. The hysteresis in the compression/decompression results may be explained by conformation changes in the surface layer that may also involve desorption and reabsorption. Upon compression, the polymer molecules are reorganized from an “optimum” conformation on the surface to a slightly less surface-active conformation. In this process, some chain desorption is also taking place. The latter can be deduced from the shape of the compression curve, as the curvature is changing sign from negative to positive. If the desorption involves whole molecules or only parts of the polymer chains is uncertain, but most probably it only involves single hydrophobic blocks according to the assumed adsorption mechanism (see Appendix). In any case there must be less hydrophobic blocks in contact with the surface at the very high pressures  $> 40 \text{ mN m}^{-1}$ . When the surface area again is increased up to the initial value and further beyond, the polymer molecules are in the less surface-active conformation that results in a lower surface pressure at a given area. This reorganization is clearly reversible, so that the original optimum conformation may be restored upon the decompression, followed by a new compression back to the original drop. After recompression, the optimum configuration is not restored immediately but takes some time to equilibrate as  $\Pi$  first decreases slightly and then increases to the original optimum value. This increase probably involves readsorption of the desorbed hydrophobic blocks. All the polymers investigated in this work show this type of hysteresis.

The slope from the compression/decompression curves may be used to calculate a value for the Gibbs elasticity,  $E_0$ , according to eq 8 which may be compared to the elastic module,  $E'$ , obtained from the bubble oscillations. Such a comparison is given in Figure 11 for the 05M2D3.2 sample. The two methods seem to give corresponding values at medium surface pressures but diverge at the either low- or high-pressure end. This behavior is not surprising taking the hysteresis effect into account, because the polymer layer is further removed from its optimum configuration at either end of the compression/decompression cycle. As  $E'$  is measured only by very small oscillations around the equilibrium state, it is believed that  $E'$  is a better measure for the state of the polymer layer.

## Conclusion

The multiblock copolymers investigated in this work all show slow but quite strong adsorption behaviors. Unfolding of the polymer close to the surface and the penetration of individual hydrophobic blocks into the surface most probably control adsorption. This leads to a brush-shaped adsorption layer with hydrophobic anchor groups and hydrophilic loops protruding into the solvent. This surface layer gives very high surface dilatational elasticities and almost no viscosity. The elasticity is practically independent of polymer structure and is proportional to the surface pressure. The model based on scaling theory describes this behavior very well and makes it possible to calculate the  $\nu$  factor for the surface layer.

**Acknowledgment.** This work was supported by the Norwegian Research Council. We thank F. Candau, Institute Charles Sadron, Strasbourg, France, and her group for the generous supply of DiHexAM–AM copolymers.

## Appendix. Adsorption Mechanism

The very slow increase in the surface pressure indicates that the adsorption of these polymers is not diffusion-controlled but more likely controlled by a slow unfolding and reorientation of the polymer molecules at the surface. In this appendix we will give further evidence in favor of this conclusion.

In the process of adsorption of these block copolymers there are several steps that may be imagined: (1) the diffusion of the molecules to the subsurface, (2) breakage of inter- and intramolecular associations, (3) adsorption of hydrophobic blocks from the subsurface to the surface, and (4) possible formation of associations in the surface layer. The possibility of adsorption of hydrophilic chains is disregarded as the pure PAM polymer shows very little adsorption.

A diffusion-controlled adsorption mechanism may be expressed by the well-known rate expression obtained from Fick's second law.<sup>40,41</sup> In integrated form, supposing  $C$  is constant, the expression for the surface concentration,  $\Gamma$ , is

$$\Gamma = 2C(Dt/\pi)^{1/2} \quad (\text{A1})$$

Here  $t$  is the time,  $C$  is the bulk concentration,  $D$  is the diffusion coefficient, and  $\pi = 3.14$ . A diffusion-controlled adsorption mechanism will be expected to give a straight line in a plot of  $\Gamma$  vs  $t^{1/2}$ . In these experiments, the direct connection between  $\Gamma$  and  $t$  cannot be measured, but a measured value of  $\Pi$  may be converted to a relative value of  $\Gamma$  by using the scaling expression, eq 5, and the calculated value of  $\gamma$  from the oscillation experiments. The unknown proportionality constant in front of the scaling expression does not influence the form of eq A1 but only the exact value of the diffusion coefficient. In Figure 12 is shown such a plot for the sample 5M1D5. The proportionality constant is set equal to 1 ( $\text{m}^2 \text{ mg}^{-1}$ ) $^\nu \text{ mN m}^{-1}$ , which implies that the surface pressure is set to 1  $\text{mN m}^{-1}$  at a surface concentration of 1  $\text{mg m}^{-2}$ . This value is typical for that found for many polymers<sup>41,42</sup> but may be incorrect in this case. This choice affects the calculation of absolute rate constant(s) but not of activation energies. It is difficult to detect any linear trend in the experimental data in Figure 12, even if the relatively large errors in  $\Gamma$  at early

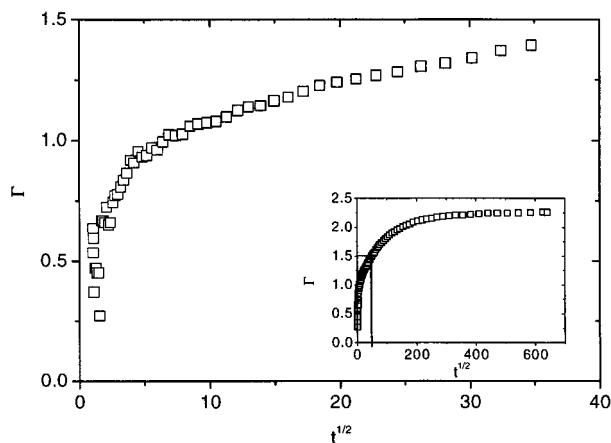


**Figure 12.** Surface excess concentration  $\Gamma$  calculated from the scaling expression (arbitrary values, see text) as a function of the square root of the time,  $t^{1/2}$ , for the copolymer 5M1D5.

times are accounted for. Using a diffusion coefficient of  $8 \times 10^{-12} \text{ m}^2 \text{ s}^{-1}$  as estimated from earlier work,<sup>24</sup> the expected straight line should be quite steep, going through maybe only the first 10–15 data points. Therefore, the conclusion may be drawn that if at all present, diffusion-controlled adsorption only operates during the first few seconds of the process.

When the adsorption is not diffusion-controlled, the concentration,  $C$ , will be the same all the way to the subsurface, and the rate-controlling step must be the activation process at the surface. This process may involve chain unfolding and breakage of inter- and intramolecular associations, reorientation, and the actual transfer to the surface. The adsorption rate may be described by a simple activation energy term by<sup>41</sup>

$$\frac{d\Gamma}{dt} = k_1 C \exp(-\epsilon/kT) \quad (\text{A2})$$

Here  $k_1$  is the adsorption rate constant, and the adsorption efficiency factor is assumed to be exponential, with  $\epsilon$  representing an activation energy,  $k$  the Boltzmann constant, and  $T$  the temperature. The desorption rate has been neglected as experimental evidence shows this to be small. A common interpretation of the activation energy is  $\epsilon = \Pi A$ .<sup>43,44</sup> With this interpretation, a plot of  $\log(d\Gamma/dt)$  against  $\Pi$  should give a straight line, and such a plot is shown in Figure 13 for three of the polymers. We see that a linear relation may be observed for quite a large part of the curve, from approximately  $\Pi > 3 \text{ mN m}^{-1}$ . The more rapid decrease in  $d\Gamma/dt$  at higher pressures may indicate a further increase in the activation energy due to a more compact surface layer. However, if we calculate the area,  $A$ , from the slopes of the lines in Figure 13, we obtain  $A = 0.99, 1.35$ , and  $1.50 \text{ nm}^2$ , respectively. If the area is interpreted as the specific molecular area, it is very low for a molecule of  $5 \times 10^5 \text{ g mol}^{-1}$ . This must mean either that the molecules in the surface layer are almost vertically oriented or that the area found here is to be interpreted as another area. The most logical choice is the specific surface area of one hydrophobic block, because the hydrophobic block adsorption must be the driving force for surface tension lowering. The fact that  $A$  increases with increasing hydrophobic block length is also in accord with this interpretation. It may therefore be surmised that adsorption is taking place one hydrophobic block at a time against an increasing surface pressure caused by the

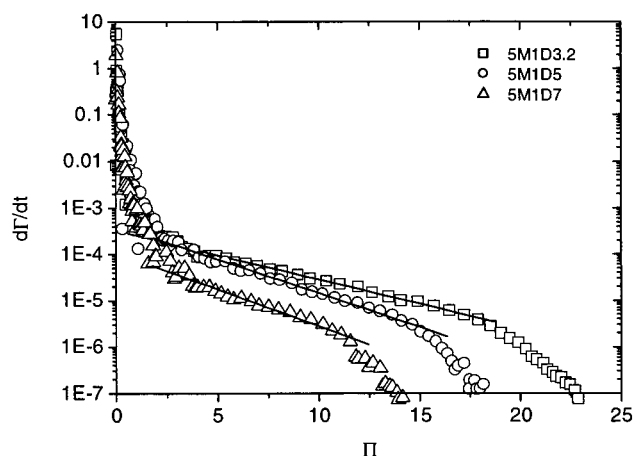


**Figure 13.**  $d\Gamma/dt$  (calculated from compression–decompression measurements) as a function of the surface pressure  $\Pi$  for the copolymers 5M1D3.2, 5M1D5, and 5M1D7 as indicated.

blocks already adsorbed. This also means that longer hydrophobic blocks, having a larger specific surface area, should adsorb more slowly when compared at the same surface pressure. This is also seen to be the case, but the difference is not very great.

The process of breakage of intramolecular associations is not expected to be dependent on the surface pressure, meaning that the rate expression for this step would not enter the  $\Pi A$  term but would be included in the adsorption constant,  $k_1$ . If we extrapolate the straight line in Figure 13 to  $\Pi = 0$ , the intercept is equal to  $k_1 C$ , and knowing  $C$ , we can calculate  $k_1$ . This value will be uncertain, however, because of the unknown absolute value of  $\Gamma$ . We see, however, that in any case the value of  $k_1$  decreases up to 5 orders of magnitude during the period when  $\Pi < 3 \text{ mN m}^{-1}$ . This means that there must be initially a very strong crowding of the surface with molecules that only have a few groups adsorbed and that further adsorption must take place by diffusion through this dense layer.

The further decrease in rate beyond ca. 12–18  $\text{mN m}^{-1}$  (dependent on hydrophobic block length) may be caused by an increasing influence in the crowding of the hydrophilic chains above the surface, thus making further adsorption still more difficult.

## References and Notes

- (1) McCormick, C. L.; Nonaka, T.; Johnson, C. B. *Polymer* **1988**, *29*, 731.
- (2) Glass, J. E. *Polymers in Aqueous Media*; ACS Symp. Ser. Vol. 223; American Chemical Society: Washington, DC, 1989.
- (3) McCormick, C. L.; Block, J.; Schulz, D. N. Water-soluble Polymers. In *Encyclopedia of Polymer Science and Engineering*; Mark, H. F., Bikales, N. M., Overberger, C. G., Menges, G., Eds.; Wiley-Interscience: New York, 1989; Vol. 17, p 730.
- (4) Iliopoulos, I.; Wang, T. K.; Audebert, R. *Langmuir* **1991**, *7*, 617.
- (5) *Macromolecular Complexes in Chemistry and Biology*; Dubin, P., Bock, J., Davies, R. M., Schulz, D. N., Thies, C., Eds.; Springer-Verlag: Berlin, 1994.
- (6) Hill, A.; Candau, F.; Selb, J. *Macromolecules* **1993**, *26*, 4521.
- (7) Renoux, D.; Selb, J.; Candau, F. *Prog. Colloid Polym. Sci.* **1994**, *97*, 213.
- (8) Candau, F.; Biggs, S.; Hill, A.; Selb, J. *Prog. Org. Coat.* **1994**, *24*, 11.
- (9) Magny, B.; Iliopoulos, I.; Zana, R.; Audebert, R. *Langmuir* **1994**, *10*, 3180.
- (10) Volpert, E.; Selb, J.; Candau, F. *Macromolecules* **1996**, *29*, 1452.
- (11) Klucker, R.; Schosseler, F. *Macromolecules* **1997**, *30*, 4927.



- (12) Thuresson, K.; Lindman, B.; Nyström, B. *J. Phys. Chem. B* **1997**, *101*, 6450.
- (13) Iversen, C.; Kjøniksen, A.-L.; Nyström, B.; Nakken, T.; Palmgren, O.; Tande, T. *Polym. Bull.* **1997**, *39*, 747.
- (14) Walderhaug, H.; Hansen, F. K.; Abrahmsén, S.; Persson, K.; Stilbs, P. *J. Phys. Chem.* **1993**, *97*, 8336.
- (15) Shaw, K. G.; Leipold, D. P. *J. Coat. Technol.* **1985**, *57*, 63.
- (16) *Polymers as Rheology Modifiers*; Schulz, D. N., Glass, J. E., Eds.; American Chemical Society: Washington, DC, 1991.
- (17) Hansen, F. K.; Nyström, B.; Walderhaug, H. *Colloids Surf. A: Phys. Eng. Aspects* **1996**, *112*, 85.
- (18) Myrvold, R.; Hansen, F. K. *J. Colloid Interface Sci.* **1998**, *207*, 97.
- (19) Myrvold, R.; Hansen, F. K.; Lindman, B. The Adsorption and Surface Dilatational Rheology of Unmodified and Hydrophobically Modified EHEC, Measured by Means of Axisymmetric Drop Shape Analysis. In *Water Soluble Polymers*; Glass, E., Ed.; ACS Symp. Ser.; American Chemical Society: Washington, DC, 2000.
- (20) Frømyr, T.; Hansen, F. K.; Kotzev, A.; Laschewsky, A. *Langmuir*, submitted.
- (21) Effing, J. J.; McLennan, I. J.; Os, N. M. v.; Kwak, J. C. T. *J. Phys. Chem.* **1994**, *98*, 12397.
- (22) Howley, C.; Marangoni, D. G.; Kwak, J. C. T. *Colloid Polym. Sci.* **1997**, *275*, 760.
- (23) Hwang, F. S.; Hogen-Esch, T. E. *Macromolecules* **1995**, *28*, 3328.
- (24) Kopperud, H. M.; Hansen, F. K.; Nyström, B. *Macromol. Chem. Phys.* **1998**, *199*, 2385.
- (25) Kopperud, H. B. M.; Walderhaug, H.; Hansen, F. K. *Macromol. Chem. Phys.* **1999**, *200*, 1839.
- (26) Regalado, E. J.; Selb, J.; Candau, F. *Macromolecules* **1999**, *32*, 8580.
- (27) Hansen, F. K.; Rødsrud, G. *J. Colloid Interface Sci.* **1991**, *141*, 1.
- (28) Hansen, F. K. *J. Colloid Interface Sci.* **1993**, *160*, 209.
- (29) Edwards, D. A.; Brenner, H.; Wasan, D. T. *Interfacial Transport Processes and Rheology*; Butterworth-Heinemann Publishers: Woburn, MA, 1991.
- (30) Dhukin, S. S.; Kretzschmar, G.; Miller, R. *Dynamics of Adsorption at Liquid Interfaces*; Elsevier: Amsterdam, 1995.
- (31) Lucassen-Reynders, E. H. *Surfactant Sci. Ser.* **1981**, *11*, 173.
- (32) Lucas, E. F.; Silva, C. X.; Pereira, G. S. *Polym. Bull.* **1997**, *39*, 73.
- (33) Zhang, J.; Pelton, R. *J. Polym. Sci., Part A: Polym. Chem.* **1999**, *37*, 2137.
- (34) Joos, P.; Fainerman, V. B. *Dynamic Surface Phenomena*; Vsp: Utrecht, 1999.
- (35) Ferry, J. D. *Viscoelastic Properties of Polymers*, 3rd ed.; John Wiley & Sons: New York, 1980.
- (36) Vilanove, R.; Poupinet, D.; Rondelez, F. *Macromolecules* **1988**, *21*, 2880.
- (37) Jiang, Q.; Chiew, Y. C. *Macromolecules* **1994**, *27*, 32.
- (38) Takahashi, A.; Yoshida, A.; Kawaguchi, M. *Macromolecules* **1982**, *15*, 1196.
- (39) Kulicke, W. M.; Kniewske, R.; Klein, J. *Prog. Polym. Sci.* **1982**, *8*, 373.
- (40) MacRitchey, F. *Chemistry at Interfaces*; Academic Press: San Diego, 1990.
- (41) Hansen, F. K.; Myrvold, R. *J. Colloid Interface Sci.* **1995**, *176*, 498.
- (42) Myrvold, R.; Hansen, F. K.; Balinov, B. *Colloids Surf. A: Phys. Eng. Aspects* **1996**, *117*, 27.
- (43) MacRitchey, F.; Alexander, A. E. *J. Colloid Interface Sci.* **1963**, *18*, 453.
- (44) Subirade, M.; Gueguen, J.; Schwenke, K. D. *J. Colloid Interface Sci.* **1992**, *152*, 442.

MA002079Y